Unanchoring the Mind: DAE-Guided Counterfactual Reasoning for Rare Disease Diagnosis

Yuting Yan[1] **Yinghao Fu**[1,2] **Wendi Ren**[1]

Shuang Li[1,*]
[1]School of Data Science, The Chinese University of Hong Kong (Shenzhen)
[2]Department of Biostatistics, City University of Hong Kong
lishuang@cuhk.edu.cn
*Corresponding author

Abstract

Diagnosing rare diseases remains a persistent challenge, often hindered by *cognitive anchoring*: once clinicians settle on a common diagnosis, alternative-especially rare-explanations are often dismissed. To address this, we propose a human-centered counterfactual reasoning framework using a Denoising Autoencoder (DAE) to simulate *what-if* diagnostic scenarios that disrupt clinicians' initial assumptions. Our model uniquely jointly learns (1) the true distribution of diseases and symptoms, and (2) human diagnostic behavior, revealing critical gaps between *medically possible* and *clinically considered* diagnoses. By strategically perturbing latent patient representations, it generates *contrastive counterfactuals* that highlight rare-but-plausible conditions—conditions typically overlooked due to cognitive bias. Unlike traditional decision-support tools, our system *proactively* suggests rare diseases not because they are statistically probable, but because they are *cognitively neglected*. Evaluated on three rare disease datasets, our approach outperforms standard machine learning classifiers in detecting rare conditions while maintaining strong performance on common diagnoses. Beyond boosting accuracy, it fosters *hypothesis-driven reasoning*, enhancing both diagnostic precision and clinician learning.

1 Introduction

Despite advances in machine learning for clinical diagnosis, *rare diseases remain notoriously difficult to identify* due to their low prevalence, heterogeneous manifestations, and frequent overlap with more common conditions [Schieppati et al., 2008, Griggs et al., 2009]. Consider a patient presenting with persistent fatigue, joint pain, and skin rashes, clinicians often anchor on familiar diagnoses like lupus rather than considering rare alternatives such as Ehlers-Danlos syndrome. This diagnostic misdirection is not merely a result of statistical rarity or symptom ambiguity, but also due to a well-documented *cognitive bias* known as *anchoring*—clinicians' tendency to settle prematurely on an initial diagnosis and insufficiently revise it in light of new or contradictory evidence [Tversky and Kahneman, 1974, Saposnik et al., 2016, Croskerry, 2002, Li et al., 2023].

This *cognitive anchoring* introduces a significant bottleneck in *rare disease detection*, often leading to prolonged diagnostic delays, repeated misdiagnoses, and unnecessary interventions. Studies in clinical cognition have shown that medical decision-making is often driven by fast, heuristic-based thinking that prioritizes pattern recognition over analytical reassessment [Norman et al., 2024]. This is especially problematic in the context of rare diseases, where diagnostic presentations often overlap with more common syndromes, creating fertile ground for premature closure. While previous

39th Conference on Neural Information Processing Systems (NeurIPS 2025) Workshop: The Second Workshop on GenAI for Health: Potential, Trust, and Policy Compliance.

machine learning efforts have primarily focused on enhancing accuracy through larger datasets or more powerful models [Juba and Le, 2019, Sun et al., 2017, Moreno-Barea et al., 2020], few have addressed the cognitive constraints that shape clinicians' interactions with model predictions, particularly under uncertainty. Moreover, existing studies indicate that clinicians may be unable to effectively integrate the AI's reasoning due to its opaque recommendations [Jussupow et al., 2021, Lebovitz et al., 2022], potentially exacerbating misdiagnoses [Jussupow et al., 2022].

Our work tackles the dual challenge of data sparsity and cognitive rigidity by introducing a diagnostic framework that not only *detects rare diseases* but also *mitigates the cognitive biases*—particularly *anchoring*—that hinder accurate diagnosis. Instead of merely maximizing predictive likelihood, our system acts as a cognitive aid, encouraging clinicians to consider alternative diagnostic hypotheses. Drawing from cognitive science theories of bias mitigation [Croskerry, 2002] and leveraging recent advances in generative modeling, we design a Denoising Autoencoder (DAE) [Vincent et al., 2008] generative model to generate plausible diagnostic counterfactuals that promote reflective reasoning.

Our DAE-based model is trained on annotated clinical data to learn both disease distributions and typical diagnostic behaviors. By perturbing the latent representation of a patient's profile, the model generates alternative diagnostic paths—plausible yet cognitively overlooked possibilities—that suggest*follow-up tests*, outside the clinician's immediate expectations. For example, it might suggest:

> *The most likely rare disease overlapping with the current symptoms is* ***Ehlers-Danlos syndrome****. Consider additional tests such as* ***genetic screening*** *for connective tissue disorders. If the results are* ***positive****, the probability of this diagnosis* ***increases significantly****.*

Unlike traditional AI systems that deliver static predictions, our framework promotes active cognitive engagement, helping clinicians*break habitual diagnostic patterns* and *rethink their assumptions*. By surfacing rare yet plausible conditions, it expands the diagnostic space, fosters reflective thinking, and supports more informed clinical decisions. As [Buçinca et al., 2021] have demonstrated, a mechanism that guides users to actively engage in critical thinking about initial assumptions enhances decision-making quality more effectively than merely providing predictions.

In our experiments, we evaluate the system's effectiveness using three rare disease datasets. our method outperformed conventional machine learning (ML) classifiers in rare disease detection while preserving optimal performance on common disease diagnosis. Counterfactual *validation* was performed by comparing the model's hypotheses with diagnoses made by *human clinicians* and assessments from *Large Language Models (LLMs).* The results confirmed that our model could identify plausible but cognitively neglected conditions, thereby enhancing diagnostic precision and fostering clinician learning.

2 Inherent Challenges in Modeling Rare Disease Diagnosis

In clinical diagnosis, the fundamental task is to infer the underlying disease label $Y \in \mathcal{Y}$ from observed clinical evidence $X \in \mathcal{X}$, such as patient-reported symptoms. Both human clinicians and ML models aim to learn or approximate the mapping:

$$h : X \mapsto \hat{Y}, \quad \text{where } \hat{Y} \approx \arg\max_{Y} P(Y \mid X).$$

By Bayes' theorem, this conditional probability can be expressed as:

$$P(Y \mid X) = \frac{P(X \mid Y) \cdot P(Y)}{P(X)},$$

where $P(Y)$ encodes prior knowledge of disease prevalence and $P(X \mid Y)$ reflects the data-generating process (e.g., symptom presentation) conditioned on a specific disease. However, in the context of *rare disease diagnosis*, this inferential process becomes fundamentally challenging, no matter for logistic regression, support vector machines, or even deep classifiers, are all subject to the same three critical limitations:

1. **Skewed priors.** Rare diseases typically have extremely small $P(Y)$. This prior imbalance biases both clinicians and ML models to favor common diagnoses, even when rare diseases are more plausible explanations.
2. **Overlapping symptom profiles.** Many hallmark symptoms of rare diseases (e.g., fatigue, muscle pain, or inflammation) are nonspecific and widely shared across common conditions. As a result, the likelihoods $P(X \mid Y_{\text{rare}})$ and $P(X \mid Y_{\text{common}})$ often overlap significantly, making discrimination between them highly uncertain.

3. **Incomplete evidence.** Key diagnostic features—such as genetic markers or specialized imaging—are frequently missing from the record, due to cost, lack of access, or simply being overlooked. This leads to an underspecified X, causing both humans and machines to rely on incomplete or biased feature sets. Such gaps often *reinforce* cognitive heuristics like *anchoring*, where initial impressions dominate the diagnostic path.

These challenges create a shared *algorithmic–cognitive bottleneck* across both humans and machines. Standard discriminative models $h : X \mapsto Y$, trained to directly map observed features to labels, inherit the same structural vulnerabilities as their human counterparts. Without mechanisms to uncover latent structures, handle missing information, or actively de-bias the inference process, both fall short in the critical task of detecting rare and underrepresented diseases.

2.1 Motivation for a Latent-State Generative Model

These insights motivate the need for a new kind of AI-aided diagnostic framework—one that can:

- *Explicitly identify cases where the observed X lies in an ambiguous or overlapping region* of the feature space;
- *Hypothesize possible latent rare disease explanations* even when current evidence is incomplete;
- *Proactively recommend additional complementary tests* (e.g., genetic panels, imaging) that can disambiguate competing diagnoses and help clinicians *break out of anchored diagnostic pathways*.

A discriminative model alone cannot meet these goals, as it is designed only to map observed input X to a label prediction $\hat{Y}$ and lacks any mechanism for reasoning about uncertainty, missing data, or counterfactual information acquisition. To address these limitations, we propose a *latent-state generative model* based on the Denoising Autoencoder (DAE) framework. This model explicitly learns a latent representation Z of the patient's symptom input X and generates possible reconstructions and diagnostic outcomes in a controlled, interpretable manner. The goal is to assist both machine and human diagnostic reasoning by generating alternative hypotheses—especially those corresponding to rare conditions that might be missed due to low priors or heuristic bias.

The proposed latent-state generative model takes the following form (as illustrated in Figure.1):

- **Input:** X (observed patient symptoms)
- **Latent state:** Z (learned stochastic representation of patient condition)
- **Outputs:**
  1. X': A reconstructed or generated version of patient symptoms (counterfactual or prototypical symptom set)
  2. $\hat{Y}^{\text{AI}}$: Prediction of the true diagnosis based on latent state Z
  3. $\hat{Y}^{\text{human}}$: Model's simulation of a human doctor's likely diagnostic decision

3 Our Proposed Generative Model Formulation

We assume access to a dataset of triplets $\left\{\left(X_i, Y_i^{\text{human}}, Y_i^{\text{true}}\right)\right\}_{i=1}^{N}$, where $X_i \in \mathbb{R}^d$ represents patient features, $Y_i^{\text{true}} \in \{1, \ldots, C\}$ is the ground-truth diagnosis, and Y_i^{human} is the clinician's recorded label. Our goal is to learn a generative latent-state model that captures three components: the patient's latent diagnostic state Z, the clinician's decision Y^{human}, and the AI's prediction Y^{AI}. By explicitly modeling the cognitive gap between human and AI reasoning, the model enables discrepancy-aware inference and supports bias-aware diagnostic support.

$$p_\theta\left(X, Y^{\text{AI}}, Y^{\text{human}}, Z\right) = p(Z) p_\theta(X \mid Z) p_\theta\left(Y^{\text{AI}} \mid Z\right) p_\theta\left(Y^{\text{human}} \mid \tilde{Z}\right) \tag{1}$$

Here, $Z \in \mathbb{R}^k$ is a latent representation inferred from X, and $\tilde{Z}$ denotes a modulated version of Z. Although humans and AI observe the same input X, their predictions can diverge due to: (1) cognitive load limiting human attention to parts of X, and (2) fundamentally different mapping functions. We explicitly reflect these factors in the design of our DAE-based generative model.

Latent Representation Learning with Masked Denoising Autoencoder Given that real-world clinical inputs $X \in \mathbb{R}^d$ often contain missing or underreported features, particularly for rare diseases, we employ a masked Denoising Autoencoder (mDAE) [Dupuy et al., 2024] strategy, to learn a robust and informative latent representation Z.

For each observed input X_i, we sample a binary mask $r_i \in \{0, 1\}^d$ to randomly drop a subset of observed entries, simulating incomplete or noisy records. The resulting corrupted input is $\tilde{X}_i =$

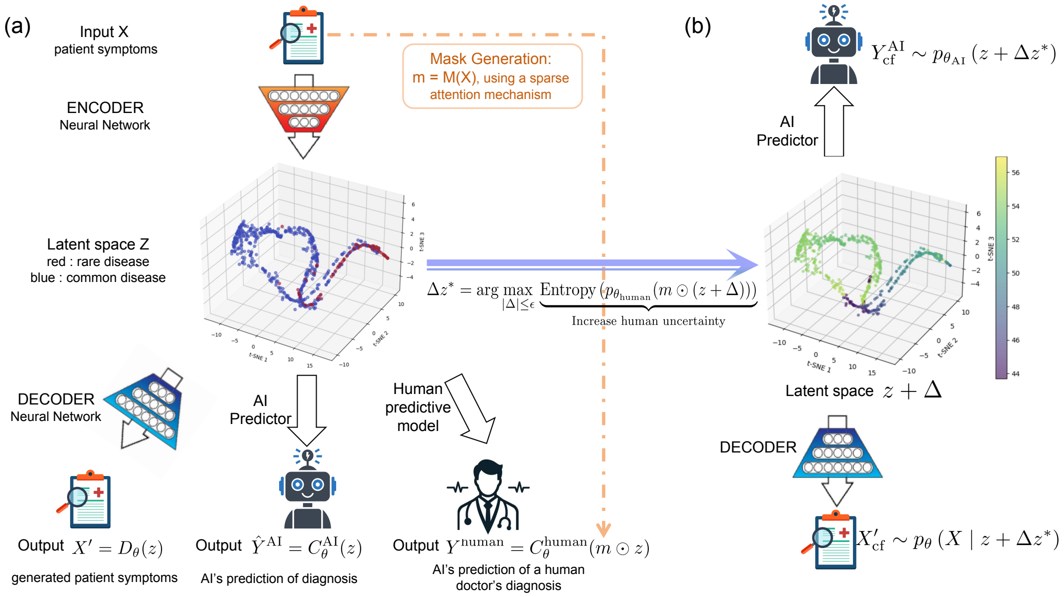
(a)
Input X
patient symptoms
ENCODER
Neural Network
Mask Generation:
m = M(X), using a sparse attention mechanism
Latent space Z
red : rare disease
blue : common disease
t-SNE 1
t-SNE 2
t-SNE 3
DECODER
Neural Network
AI Predictor
Human predictive model
Output $X' = D_\theta(z)$
generated patient symptoms
Output $\hat{Y}^{\mathrm{AI}} = C_\theta^{\mathrm{AI}}(z)$
AI's prediction of diagnosis
Output $Y^{\mathrm{human}} = C_\theta^{\mathrm{human}}(m \odot z)$
AI's prediction of a human doctor's diagnosis
$\Delta z^* = \arg\max_{|\Delta|\leq\epsilon} \underbrace{\mathrm{Entropy}\left(p_{\theta_{\mathrm{human}}}(m \odot (z+\Delta))\right)}_{\text{Increase human uncertainty}}$
(b)
$Y_{\mathrm{cf}}^{\mathrm{AI}} \sim p_{\theta_{\mathrm{AI}}}(z + \Delta z^*)$
AI Predictor
Latent space $z + \Delta$
DECODER
$X'_{\mathrm{cf}} \sim p_\theta(X \mid z + \Delta z^*)$

Figure 1: DAE-guided counterfactual reasoning framework. (a) DAE encodes patient features into a latent space, enabling dual predictors for AI and clinician diagnoses. (b) Counterfactuals are generated by perturbing latent vectors to increase uncertainty in human model. Then AI predictor can generate counterfactual diagnosis and decoder reconstructs the corresponding patient profile.

$r_i \odot X_i$, which is then encoded to a latent distribution $q_\phi\left(Z_i \mid \tilde{X}_i\right)$. The decoder reconstructs the full input, and the reconstruction loss is computed only on the originally observed (i.e., uncorrupted) entries:

$$\mathcal{L}_{\text{recon}} = \mathbb{E}_{q_\phi(Z_i|\tilde{X}_i)}\left[\left\|(1-r_i)\odot\left(X_i - \hat{X}_i\right)\right\|_2^2\right] \tag{2}$$

This approach helps the model infer missing or overlooked features—like masked token prediction in language models—while learning robust, task-relevant representations. These generalizable embeddings enable effective downstream applications such as diagnosis prediction and modeling human-AI divergence.

Dual Classification Losses The latent code Z_i is leveraged to predict two diagnostic outcomes: the *ground-truth diagnosis* Y_i^{true}, and the *observed human diagnosis* Y_i^{human}.
We define two separate classification objectives:

- **AI Prediction Loss (truth-matching):**

$$\mathcal{L}_{\text{AI}} = -\mathbb{E}_{q_\phi(Z_i|X_i)}\left[\sum_c \alpha_c(1-p_c)^\gamma \log p_c\right], \quad \alpha_c \propto \frac{1}{\text{freq}(c)} \tag{3}$$

Here, $p_c = p_{\theta_{\text{AI}}}(Y_i^{\text{true}} = c \mid Z_i)$ denotes the predicted probability of class c under the AI classifier. This objective encourages the model to leverage the *full latent representation* Z_i to generate accurate, clinically grounded predictions aligned with the ground-truth diagnosis, using a classifier parameterized by θ_{AI}.

To address class imbalance-particularly prevalent in rare disease settings, we employ a focal loss variant [Lin et al., 2017] that dynamically down-weights well-represented, easily classified categories and emphasizes learning from rare or ambiguous cases. As the system is intended to assist clinicians in complex diagnostic scenarios, this calibrated formulation promotes more *exploratory* AI behavior, enabling the model to surface atypical or underrecognized patterns that may otherwise be overlooked. Thus, the AI acts not only as a predictor but also as a discovery aid, supporting more comprehensive and inclusive clinical decision-making.

- **Human Simulation Loss (cognitive-matching):**

$$\mathcal{L}_{\text{human}} = \mathbb{E}_{q_\phi(Z_i|X_i)}\left[-\log p_{\theta_{\text{human}}}\left(Y_i^{\text{human}} \mid \tilde{Z}_i\right)\right] \tag{4}$$

Here, $\tilde{Z}_i = m_i \odot Z_i$ is a selectively masked version of the latent vector, where the learned attention mask $m_i \in [0,1]^k$ gates which latent dimensions are used by the human prediction head. This reflects the idea that, given the same input X_i, *humans and AI may focus on different parts of the data and apply distinct cognitive functions to reach a diagnosis*.

Importantly, the prediction functions for AI and human simulation are parameterized separately, using θ_{AI} and θ_{human} respectively. This architectural asymmetry captures both attentional differences (via m_i) and functional differences in diagnostic reasoning, allowing us to explicitly model and analyze human-AI cognitive divergence.

Modeling Human-AI Cognitive Gaps via Sparse Self-Attention Mask Specifically, we compute the attention mask m_i using a learnable self-attention module:

$$m_i = \text{Softmax}\left(\frac{Q(X_i)\,K(X_i)^\top}{\sqrt{d}}\right) V(X_i) \tag{5}$$

where $Q(\cdot), K(\cdot), V(\cdot)$ are linear projections (as proposed in [Vaswani et al., 2017]) that produce query, key, and value vectors from the input X_i, and the output is pooled to form a k-dimensional attention vector. This attention mechanism identifies which latent features humans are likely to focus on, given the current case.

To ensure interpretability and mimic human cognitive constraints, we impose an ℓ_1 sparsity penalty on the attention mask:

$$\mathcal{L}_{\text{mask}} = \lambda_{\text{mask}} \cdot \|m_i\|_1 \tag{6}$$

This encourages the human prediction head to rely on a small subset of salient features, reflecting *limited cognitive bandwidth* and enhancing the *interpretability* of human diagnostic pathways.

Contrastive Learning for Rare Disease Separability To prevent rare disease embeddings from collapsing into common clusters, we introduce a contrastive loss:

$$\mathcal{L}_{\text{contrast}} = \sum_{(i,j,k)} \max\big(0,\ \delta + d(Z_i, Z_j) - d(Z_i, Z_k)\big),$$

where Z_i and Z_j are latent representations from the same rare disease class, and Z_k is from a common disease class.

This loss encourages embeddings of the same rare class to remain close while pushing them away from embeddings of common classes, thereby promoting greater separability and preserving the distinctiveness of rare conditions in the latent space.

Cognitive Gap Identification: Discrepancy Between AI and Human Attention To quantify the cognitive discrepancy between AI and human reasoning—especially in rare disease cases—we introduce a *cognitive gap loss*. This loss encourages the AI model to attend to features that may be under-utilized by human clinicians, highlighting potential diagnostic blind spots. Formally, we define the loss as:

$$\mathcal{L}_{\text{gap}} = \sum_{i:\, Y_i^{\text{true}} \in \text{rare}} \left\| m_i \odot \nabla_{Z_i} \log p_{\theta_{\text{AI}}}(Y_i^{\text{true}} \mid Z_i) \right\|_2^2,$$

where Z_i is the latent representation, $m_i \in [0,1]^k$ is the learned attention mask approximating human focus, and $\nabla_{Z_i} \log p_{\theta_{\text{AI}}}(Y_i^{\text{true}} \mid Z_i)$ captures the sensitivity of the AI's prediction to each latent feature.

By penalizing high-gradient regions aligned with human attention m_i, the model is encouraged to focus on dimensions that are often overlooked, especially in the context of rare diseases. This fosters attentional divergence in rare disease cases, where the AI can uncover atypical patterns that clinicians might miss due to cognitive biases.

3.1 Total Objective and Training Curriculum

The overall loss function is defined as:

$$\mathcal{L}_{\text{total}} = \mathcal{L}_{\text{rec}} + \mathcal{L}_{\text{AI}} + \mathcal{L}_{\text{human}} + \gamma\mathcal{L}_{\text{contrast}} + \eta\mathcal{L}_{\text{mask}} + \xi\mathcal{L}_{\text{gap}}\,. \tag{7}$$

The training process follows a staged curriculum, starting with the DAE warm-up using reconstruction loss, followed by the introduction of focal loss for rare disease prediction. The curriculum then adds human cognitive modeling and sparsity regularization, followed by contrastive learning for separating rare and common diseases. Finally, the cognitive gap loss is incorporated to address attention mismatches between AI and human clinicians.

We will train the DAE using the above loss function. Given the learned generative DAE model, we can design the following counterfactual generation tasks.

4 Counterfactual Generation for Cognitive Anchoring Correction

To mitigate diagnostic errors from cognitive anchoring, we introduce a counterfactual generation mechanism that leverages the model's probabilistic structure. Given patient data X, *if* $p_{\theta_{\mathrm{AI}}}$ *assigns relatively high probability to a plausible diagnosis* Y_{AI}*—particularly a rare or under-considered one—that diverges from the human's current diagnosis*, this *triggers counterfactual generation* to challenge the initial decision of human and guide follow-up evaluation or testing.

The **goal** of the counterfactual generation here is to

> *Disrupt doctors' fixation on initial hypotheses by generating alternative diagnostic pathways, particularly for rare diseases.*

Learning Optimal Perturbation The perturbation is learned to increase uncertainty in the human (or human-approximating) model, thus exposing cognitive blind spots.

$$\Delta z^* = \arg\max_{\|\Delta\|\leq\epsilon} \underbrace{\text{Entropy}\left(p_{\theta_{\text{human}}}(m \odot (z+\Delta))\right)}_{\text{Increase human uncertainty}} \tag{8}$$

Here, $\|\Delta\| \leq \epsilon$ ensures that the changes remain within a medically interpretable range. Without perturbation, the Al's prediction from the original z may align closely with the clinician's current belief. By contrast, perturbing z explores latent variations that introduce diagnostic ambiguity from the human's perspective-potentially uncovering under-recognized or rare conditions.

Counterfactual Output Generation Once the optimal perturbation Δz^* is obtained, the system generates two outputs:

- **Al Counterfactual Diagnosis**

$$Y_{\mathrm{cf}}^{\mathrm{AI}} \sim p_{\theta_{\mathrm{AI}}}(z+\Delta z^*) \tag{9}$$

This may yield a rare disease prediction that prompts reconsideration of the original diagnosis.

- **Synthetic Patient Data Generation** An mDAE is used to reconstruct the corresponding patient profile:

$$X_{\mathrm{cf}}' \sim p_\theta(X \mid z+\Delta z^*) \tag{10}$$

Here, X_{cf}' represents a plausible synthetic patient who presents similarly but includes key missing symptoms supporting the rare disease.

Finally, the system communicates the counterfactual insight as:

> *"Consider alternative diagnoses with similar presentations: [Al-suggested disease* $Y_{\mathrm{cf}}^{\mathrm{AI}}$*]. If additional findings such as* X_{cf}' *were observed, the likelihood of this condition would increase to* $p_{\theta_{\mathrm{AI}}}(Y_{\mathrm{cf}}^{\mathrm{AI}} \mid z+\Delta)$*."*

This form of explanation aims to encourage the clinician to reflect, reassess, and refine their diagnostic reasoning with evidence-informed support from the AI.

5 Experiment

To evaluate the effectiveness of our proposed framework, we conducted extensive experiments designed to (i) validate robust performance and diagnostic accuracy for *rare disease* detection and (ii) assess the efficacy of counterfactual explanations in addressing cognitive gaps and guiding clinical decision-making.

We used three private, real-world *rare disease* datasets that we constructed and curated in close collaboration with a top-tier hospital, involving multiple departments and clinicians, covering **Gitelman syndrome**, **acromegaly**, and **hypertrophic cardiomyopathy (HCM)**. To support reproducibility, we additionally evaluate on a curated public rare disease dataset for **Granulomatosis with Polyangiitis (GPA)** derived from [Chen et al., 2024]. Detailed dataset specifications are provided in Appendix B. Notably, High-quality datasets for rare diseases are scarce, and assembling high-quality rare disease datasets with research value is inherently challenging and constitutes a substantive contribution to the field.

5.1 Representational and Predictive Capacity

5.1.1 Prediction on Imbalanced Data

The low prevalence of rare diseases leads to imbalanced datasets, posing challenges for conventional classifiers. We present results on a real-world Gitelman syndrome dataset, which has faced difficulties in predicting this disease, with an imbalance ratio of 94:100 to 94:500 (rare disease samples to common disease samples). Standard class-imbalance handling strategies were applied to all baselines, including focal loss for the neural network, SMOTE augmentation for SVM and logistic regression, and built-in imbalance handling for XGBoost and LightGBM.

Our approach outperforms five typical classifiers, as shown in Figure 2, which reports AUC, accuracy for common diseases, and rare disease accuracy. Notably, our model's AUC improves with increasing imbalance, as the larger data volume provides more information for learning despite the greater skew.

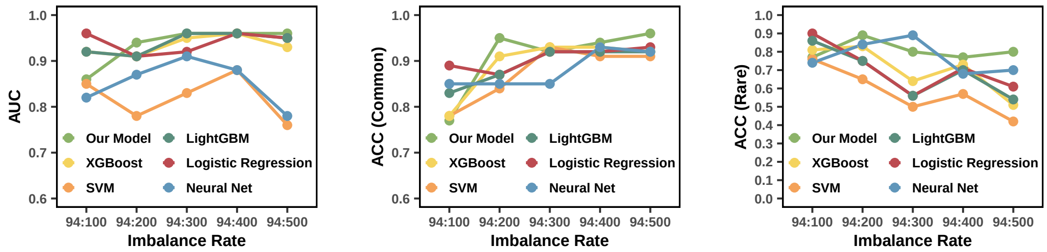

Figure 2: Comparison of model performance under imbalanced data.

5.1.2 Latent Space Visualization

We visualize the model's latent space using the Gitelman dataset in three distinct ways. These visualizations, shown in Figure. 3, offer valuable insights into the model's internal representations. Panel (a) shows the structural organization of latent embeddings, illustrating the model's ability to encode fine-grained phenotypic details that distinguish clinically similar samples. Panel (b) presents an attention map of clinician focus within the same space: mask values of 1 mark high clinical relevance regions, while 0 indicates lower priority, directly aligning attention with diagnostic importance. Panel (c) highlights features exerting significant influence on human classification decisions, exposing potential decision boundaries where predictions may shift. The visualization principle involves perturbing latent space vectors to maximize human prediction uncertainty, with the intensity distribution directly reflecting perturbation magnitude. Lighter colors denote higher diagnostic uncertainty, revealing critical knowledge gaps that could lead to misdiagnosis.

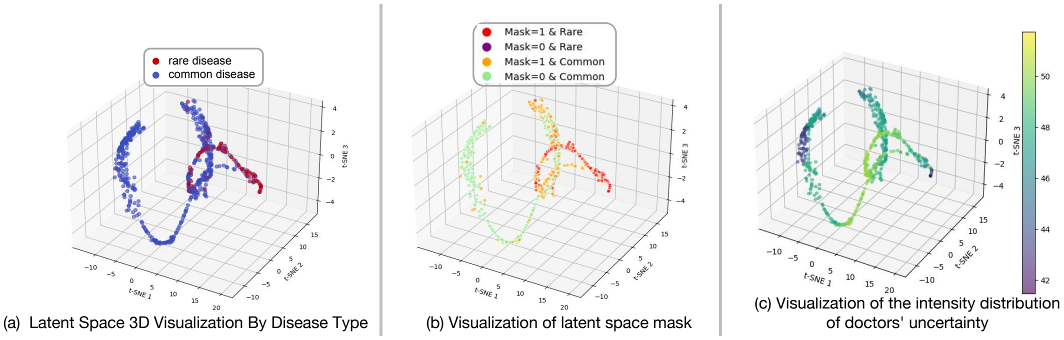

(a) Latent Space 3D Visualization By Disease Type

(b) Visualization of latent space mask

(c) Visualization of the intensity distribution of doctors' uncertainty

Figure 3: Latent space visualization by disease type, clinician attention, and diagnostic uncertainty.

5.1.3 Ablation Visualization

We also examine how each loss term in the fine-tuning stage shapes the latent space via an ablation study, with key findings visualized in Fig. 4. Specifically, removing the contrastive, gap, or reconstruction loss degrades the quality of latent space representations, thereby impairing the model's ability to distinguish similar samples; in contrast, removing the prediction or mask-regularization loss undermines the performance of AI/human predictors, as evidenced by lower AUC scores and corresponding visualizations presented in the figure.

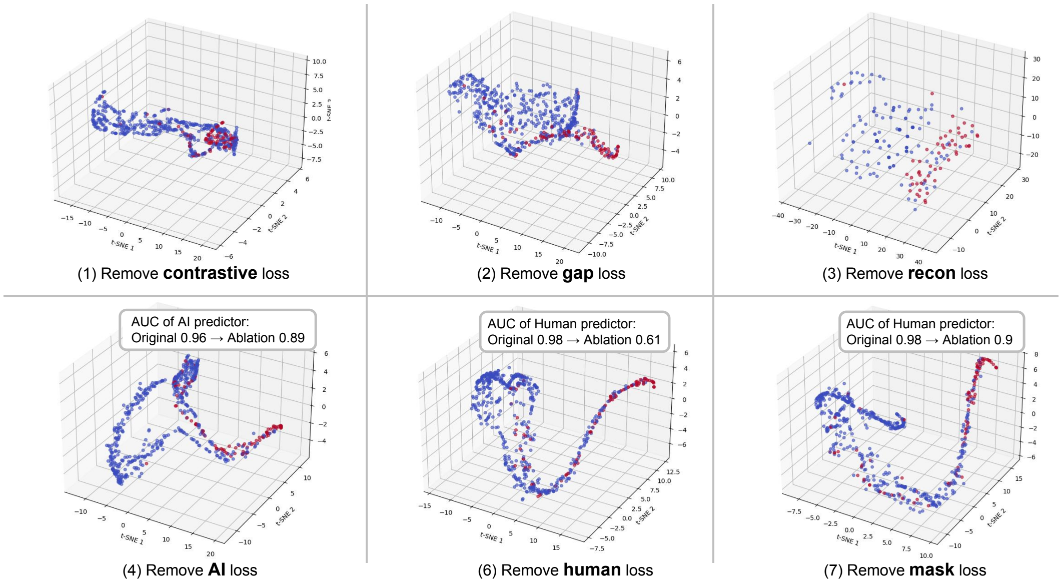

(1) Remove **contrastive** loss

(2) Remove **gap** loss

(3) Remove **recon** loss

AUC of AI predictor:
Original 0.96 → Ablation 0.89

(4) Remove **AI** loss

AUC of Human predictor:
Original 0.98 → Ablation 0.61

(6) Remove **human** loss

AUC of Human predictor:
Original 0.98 → Ablation 0.9

(7) Remove **mask** loss

Figure 4: Ablation study: loss function removal impact on latent space and model performance.

5.1.4 AUC Across Datasets and Ablation Experiments

We also report AI and human predictors' AUC across 4 datasets (10-run avg ± std, Table 1). The full model shows consistent strong performance, demonstrating robust, stable generalization. Ablations (removing one loss at a time in fine-tuning, stage-wise pretraining unchanged) corroborate each component's necessity: removing AI loss notably degrades AI predictor AUC; removing human loss or mask-regularization loss severely harms human predictors. For specific details regarding the model architecture and hyperparameter selection, refer to G and F.

Table 1: AUC metrics and ablations

	Gitelman		**Acromegaly**		**HCM**		**GPA**	
	AI	**Human**	**AI**	**Human**	**AI**	**Human**	**AI**	**Human**
Original	**0.96±0.01**	**0.98±0.01**	**0.99±0.01**	**0.98±0.03**	**0.96±0.01**	**0.97±0.01**	**0.88±0.04**	**0.86±0.01**
No AI loss	0.89±0.08	N/A	0.96±0.02	N/A	0.86±0.05	N/A	0.79±0.03	N/A
No human loss	N/A	0.61±0.14	N/A	0.87±0.07	N/A	0.73±0.12	N/A	0.72±0.02
No mask loss	N/A	0.90±0.08	N/A	0.94±0.05	N/A	0.92±0.02	N/A	0.81±0.03

5.2 LLM-Human Dual Quantitative Evaluation of Counterfactuals

To address the challenges and diagnostic needs in rare disease medicine, our model supports counterfactual analysis across diverse scenarios. We constructed three representative counterfactual scenarios: **Scenario 1**: Feature Completion for Low-Confidence Predictions, **Scenario 2**: AI-Human Prediction Discrepancy Resolution, and **Scenario 3**: Uncertainty-Driven Alternative Diagnoses. For detailed descriptions of these scenarios, please refer to Appendix E.

For a more comprehensive assessment, an LLM- and doctor-based evaluation framework is designed for evaluating counterfactual outcomes. Fig. 5 shows Prompt, LLM evaluations and doctor evaluations across three scenarios.

Evaluated by LLM Since 2023, LLMs with advanced instruction-following and semantic comprehension have enabled automated evaluation [Gao et al., 2025]. In our framework, pre-trained LLMs assess counterfactuals using structured prompts, evaluating plausibility, relevance, and cognitive support across semantic, causal, and operational dimensions..

Evaluated by Doctors Clinical experts from a leading hospital validated rare disease counterfactuals for medical plausibility and clinical relevance, leveraging their domain expertise.

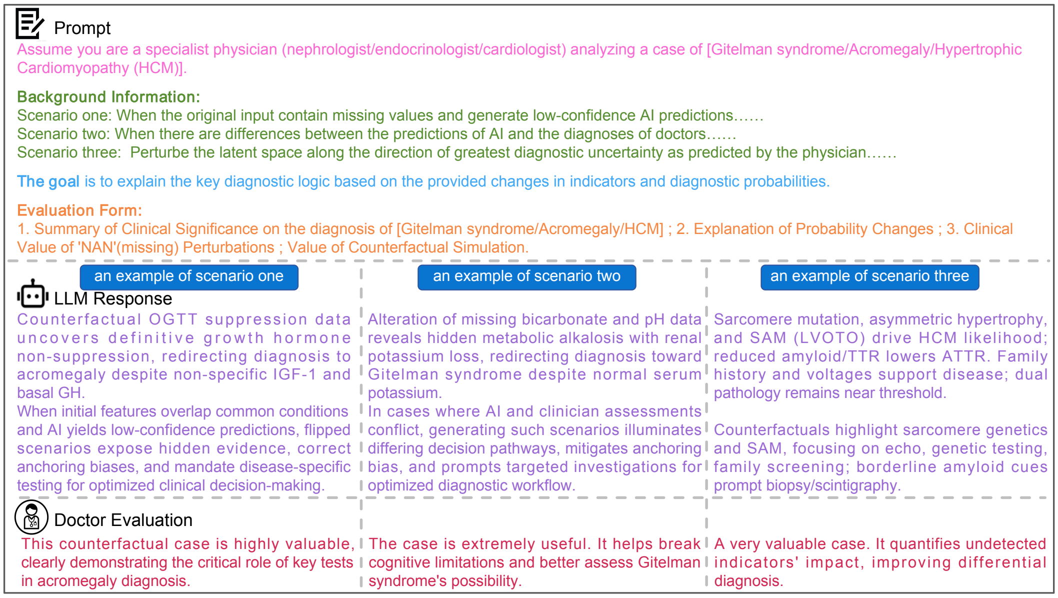

Prompt

Assume you are a specialist physician (nephrologist/endocrinologist/cardiologist) analyzing a case of [Gitelman syndrome/Acromegaly/Hypertrophic Cardiomyopathy (HCM)].

Background Information:
Scenario one: When the original input contain missing values and generate low-confidence AI predictions……
Scenario two: When there are differences between the predictions of AI and the diagnoses of doctors……
Scenario three: Perturbe the latent space along the direction of greatest diagnostic uncertainty as predicted by the physician……

The goal is to explain the key diagnostic logic based on the provided changes in indicators and diagnostic probabilities.

Evaluation Form:
1. Summary of Clinical Significance on the diagnosis of [Gitelman syndrome/Acromegaly/HCM] ; 2. Explanation of Probability Changes ; 3. Clinical Value of 'NAN'(missing) Perturbations ; Value of Counterfactual Simulation.

an example of scenario one

LLM Response

Counterfactual OGTT suppression data uncovers definitive growth hormone non-suppression, redirecting diagnosis to acromegaly despite non-specific IGF-1 and basal GH.
When initial features overlap common conditions and AI yields low-confidence predictions, flipped scenarios expose hidden evidence, correct anchoring biases, and mandate disease-specific testing for optimized clinical decision-making.

Doctor Evaluation

This counterfactual case is highly valuable, clearly demonstrating the critical role of key tests in acromegaly diagnosis.

an example of scenario two

Alteration of missing bicarbonate and pH data reveals hidden metabolic alkalosis with renal potassium loss, redirecting diagnosis toward Gitelman syndrome despite normal serum potassium.
In cases where AI and clinician assessments conflict, generating such scenarios illuminates differing decision pathways, mitigates anchoring bias, and prompts targeted investigations for optimized diagnostic workflow.

The case is extremely useful. It helps break cognitive limitations and better assess Gitelman syndrome's possibility.

an example of scenario three

Sarcomere mutation, asymmetric hypertrophy, and SAM (LVOTO) drive HCM likelihood; reduced amyloid/TTR lowers ATTR. Family history and voltages support disease; dual pathology remains near threshold.

Counterfactuals highlight sarcomere genetics and SAM, focusing on echo, genetic testing, family screening; borderline amyloid cues prompt biopsy/scintigraphy.

A very valuable case. It quantifies undetected indicators' impact, improving differential diagnosis.

Figure 5: Illustration of prompt, LLM response segment and real world doctor evaluation segment.

5.3 Quantitative Evaluation of Counterfactuals against Baselines

Baselines We compare our method with two baseline approaches: REVISE [Joshi et al., 2019], which uses optimization within a generative model's latent space, and CF-VAE [Nagesh et al., 2023], which optimizes a variational autoencoder alongside a binary prediction model.

Metrics We evaluate counterfactuals based on two metrics: (1) **Label Flip Rate**: The proportion of counterfactuals correctly classified into the target class, indicating validity. (2) **Root Mean Squared Error (RMSE)**: Measures the perturbation magnitude between the counterfactual and original input, with lower RMSE indicating higher plausibility.

Results Table 2 compares our model, REVISE, CF-VAE, and an ablation experiment across four datasets. Our model achieves the highest label flip rate and lowest RMSE, outperforming all baselines in generating valid and minimally perturbed counterfactuals.

Table 2: Performance metrics across four datasets.

	Gitelman		Acromegaly		HCM		GPA	
Model	Label Flip Rate	RMSE	Label Flip Rate	RMSE	Label Flip Rate	RMSE	Label Flip Rate	RMSE
REVISE	0.96±0.03	5.40±0.89	0.92±0.11	13.96±14.44	0.70±0.40	0.33±0.04	0.94±0.07	0.18±0.06
CFVAE	0.96±0.02	12.00±1.77	0.85±0.15	13.96±14.84	0.80±0.40	0.33±0.01	0.85±0.18	0.29±0.09
Our Model	**1.00±0.00**	**1.93±0.76**	**1.00±0.00**	**0.18±0.10**	**1.00±0.00**	**0.10±0.13**	**1.00±0.00**	**0.12±0.03**
Ablation	**1.00±0.00**	4.85±3.27	**1.00±0.00**	0.21±0.08	**1.00±0.00**	0.46±0.27	**1.00±0.00**	0.25±0.07

6 Conclusion

We introduced a human-centered counterfactual reasoning framework that perturbs latent patient representations via a DAE-based latent state generative model to counter cognitive anchoring in rare disease diagnosis. By generating realistic "what-if" scenarios, our method surfaces overlooked conditions and guides clinicians toward alternative hypotheses. A mixed LLM- and doctor-based evaluation confirms the scientific soundness and clinical relevance of the generated cases. This framework fosters reflective diagnostic reasoning, enhances interpretability, and offers a scalable tool for bridging human knowledge gaps in challenging medical scenarios.

Acknowledgments and Disclosure of Funding

This work was in part supported by the Key Program of the NSFC under grant No. 72495131, NSFC under grant No. 62206236, Shenzhen Stability Science Program 2023, Shenzhen Science and Technology Program ZDSYS20230626091302006, and Longgang District Key Laboratory of Intelligent Digital Economy Security.

References

Arrigo Schieppati, Jan-Inge Henter, Erica Daina, and Anita Aperia. Why rare diseases are an important medical and social issue. *The Lancet*, 371(9629):2039–2041, 2008.

Robert C Griggs, Mark Batshaw, Mary Dunkle, Rashmi Gopal-Srivastava, Edward Kaye, Jeffrey Krischer, Tan Nguyen, Kathleen Paulus, Peter A Merkel, et al. Clinical research for rare disease: opportunities, challenges, and solutions. *Molecular genetics and metabolism*, 96(1):20–26, 2009.

Amos Tversky and Daniel Kahneman. Judgment under uncertainty: Heuristics and biases: Biases in judgments reveal some heuristics of thinking under uncertainty. *science*, 185(4157):1124–1131, 1974.

Gustavo Saposnik, Donald Redelmeier, Christian C Ruff, and Philippe N Tobler. Cognitive biases associated with medical decisions: a systematic review. *BMC medical informatics and decision making*, 16:1–14, 2016.

Pat Croskerry. Achieving quality in clinical decision making: Cognitive strategies and detection of bias. *Academic Emergency Medicine*, 9(11):1184–1204, 2002. doi: https://doi.org/10.1197/aemj.9.11.1184. URL `https://onlinelibrary.wiley.com/doi/abs/10.1197/aemj.9.11.1184`.

Alexander C Li, Mihir Prabhudesai, Shivam Duggal, Ellis Brown, and Deepak Pathak. Your diffusion model is secretly a zero-shot classifier. In *Proceedings of the IEEE/CVF International Conference on Computer Vision*, pages 2206–2217, 2023.

Geoff Norman, Thierry Pelaccia, Peter Wyer, and Jonathan Sherbino. Dual process models of clinical reasoning: the central role of knowledge in diagnostic expertise. *Journal of Evaluation in Clinical Practice*, 30(5):788–796, 2024.

Brendan Juba and Hai S. Le. Precision-recall versus accuracy and the role of large data sets. *Proceedings of the AAAI Conference on Artificial Intelligence*, 33(01):4039–4048, July 2019. doi: 10.1609/aaai.v33i01.33014039.

Chen Sun, Abhinav Shrivastava, Saurabh Singh, and Abhinav Gupta. Revisiting unreasonable effectiveness of data in deep learning era. In *Proceedings of the IEEE international conference on computer vision*, pages 843–852, 2017.

Francisco J Moreno-Barea, José M Jerez, and Leonardo Franco. Improving classification accuracy using data augmentation on small data sets. *Expert Systems with Applications*, 161:113696, 2020.

Ekaterina Jussupow, Kai Spohrer, Armin Heinzl, and Joshua Gawlitza. Augmenting medical diagnosis decisions? an investigation into physicians' decision-making process with artificial intelligence. *Information Systems Research*, 32(3):713–735, 2021.

Sarah Lebovitz, Hila Lifshitz-Assaf, and Natalia Levina. To engage or not to engage with ai for critical judgments: How professionals deal with opacity when using ai for medical diagnosis. *Organization science*, 33(1):126–148, 2022.

Ekaterina Jussupow, Kai Spohrer, and Armin Heinzl. Radiologists' usage of diagnostic ai systems: The role of diagnostic self-efficacy for sensemaking from confirmation and disconfirmation. *Business & Information Systems Engineering*, 64(3):293–309, 2022.

Pascal Vincent, Hugo Larochelle, Yoshua Bengio, and Pierre-Antoine Manzagol. Extracting and composing robust features with denoising autoencoders. In *Proceedings of the 25th international conference on Machine learning*, pages 1096–1103, 2008.

Zana Buçinca, Maja Barbara Malaya, and Krzysztof Z Gajos. To trust or to think: cognitive forcing functions can reduce overreliance on ai in ai-assisted decision-making. *Proceedings of the ACM on Human-computer Interaction*, 5(CSCW1):1–21, 2021.

Mariette Dupuy, Marie Chavent, and Remi Dubois. mdae: modified denoising autoencoder for missing data imputation. *arXiv preprint arXiv:2411.12847*, 2024.

Tsung-Yi Lin, Priya Goyal, Ross B. Girshick, Kaiming He, and Piotr Dollár. Focal loss for dense object detection. *2017 IEEE International Conference on Computer Vision (ICCV)*, pages 2999–3007, 2017.

Ashish Vaswani, Noam M. Shazeer, Niki Parmar, Jakob Uszkoreit, Llion Jones, Aidan N. Gomez, Lukasz Kaiser, and Illia Polosukhin. Attention is all you need. In *Neural Information Processing Systems*, 2017.

Xuanzhong Chen, Xiaohao Mao, Qihan Guo, Lun Wang, Shuyang Zhang, and Ting Chen. Rarebench: can llms serve as rare diseases specialists? In *Proceedings of the 30th ACM SIGKDD conference on knowledge discovery and data mining*, pages 4850–4861, 2024.

Mingqi Gao, Xinyu Hu, Xunjian Yin, Jie Ruan, Xiao Pu, and Xiaojun Wan. Llm-based nlg evaluation: Current status and challenges. *Computational Linguistics*, pages 1–28, 2025.

Shalmali Joshi, Oluwasanmi Koyejo, Warut Vijitbenjaronk, Been Kim, and Joydeep Ghosh. Towards realistic individual recourse and actionable explanations in black-box decision making systems. *arXiv preprint arXiv:1907.09615*, 2019.

Supriya Nagesh, Nina Mishra, Yonatan Naamad, James M Rehg, Mehul A Shah, and Alexei Wagner. Explaining a machine learning decision to physicians via counterfactuals. In *Conference on Health, Inference, and Learning*, pages 556–577. PMLR, 2023.

Sandra Wachter, Brent Mittelstadt, and Chris Russell. Counterfactual explanations without opening the black box: Automated decisions and the gdpr. *Harv. JL & Tech.*, 31:841, 2017.

Ramaravind K Mothilal, Amit Sharma, and Chenhao Tan. Explaining machine learning classifiers through diverse counterfactual explanations. In *Proceedings of the 2020 conference on fairness, accountability, and transparency*, pages 607–617, 2020.

Sahil Verma, John Dickerson, and Keegan Hines. Counterfactual explanations for machine learning: A review. *arXiv preprint arXiv:2010.10596*, 2(1):1, 2020.

Min Hun Lee and Chong Jun Chew. Understanding the effect of counterfactual explanations on trust and reliance on ai for human-ai collaborative clinical decision making. *Proceedings of the ACM on Human-Computer Interaction*, 7(CSCW2):1–22, 2023.

Eleni Straitouri, Suhas Thejaswi, and Manuel Rodriguez. Controlling counterfactual harm in decision support systems based on prediction sets. *Advances in Neural Information Processing Systems*, 37: 129443–129479, 2024.

Arnaud Van Looveren and Janis Klaise. Interpretable counterfactual explanations guided by prototypes. In *Joint European Conference on Machine Learning and Knowledge Discovery in Databases*, pages 650–665. Springer, 2021.

Daniel Nemirovsky, Nicolas Thiebaut, Ye Xu, and Abhishek Gupta. Countergan: Generating counterfactuals for real-time recourse and interpretability using residual gans. In *Uncertainty in Artificial Intelligence*, pages 1488–1497. PMLR, 2022.

Stig Hellemans, Andres Algaba, Sam Verboven, and Vincent Ginis. Flexible counterfactual explanations with generative models. *arXiv preprint arXiv:2502.17613*, 2025.

Wenzhuo Yang, Jia Li, Caiming Xiong, and Steven CH Hoi. Mace: An efficient model-agnostic framework for counterfactual explanation. *arXiv preprint arXiv:2205.15540*, 2022.

Lei Xu, Maria Skoularidou, Alfredo Cuesta-Infante, and Kalyan Veeramachaneni. Modeling tabular data using conditional gan. *Advances in neural information processing systems*, 32, 2019.

A Related work

Counterfactual Explanations The evolution of counterfactual explanations has transitioned from optimizing feature perturbations [Wachter et al., 2017] to frameworks that prioritize human-AI collaboration and safety. Early methods focused on generating minimal feasible changes (e.g., DiCE [Mothilal et al., 2020]), but were criticized for ignoring user-specific constraints and real-world applicability [Verma et al., 2020]. More recent work, including [Lee and Chew, 2023], highlights the role of counterfactuals in mitigating cognitive biases. [Lee and Chew, 2023] showed that exposing users to hypothetical scenarios reduces overreliance on erroneous AI predictions, particularly among non-experts susceptible to confirmation bias. This aligns with broader findings in human-AI interaction, where explanations must balance interpretability with decision accuracy [Buçinca et al., 2021, Straitouri et al., 2024]. A significant advancement in this area is the formalization of counterfactual harm, defined as the risk that explanations may degrade human judgment. [Straitouri et al., 2024] introduced structural causal models with conformal risk control to bound harmful outcomes in clinical systems. Their approach integrates monotonicity assumptions (e.g., "higher biomarker values correlate with worse prognosis") to ensure explanations align with domain knowledge, thereby addressing a gap in earlier optimization-based methods [Van Looveren and Klaise, 2021]. This shift reflects a growing emphasis on safety-critical metrics, moving beyond traditional criteria like sparsity and realism [Verma et al., 2020].

Counterfactual Generative Models Generative models have been introduced to generate numerical counterfactuals, enabling dynamic adaptation to user constraints. Early GAN-based approaches, such as CounterRGAN [Nemirovsky et al., 2022], enforced immutable features via residual networks but lacked flexibility for real-time customization. FCEGAN [Hellemans et al., 2025] addresses this limitation by incorporating user-defined templates and dual discriminator losses, facilitating personalized explanations in domains like loan approvals [Yang et al., 2022]. These frameworks align with CTGAN's training-by-sampling strategy [Xu et al., 2019] to handle class imbalance, a persistent challenge in financial and medical datasets. While REVISE [Joshi et al., 2019] introduced a method for generating numerical counterfactuals using arbitrary generative models, it can produce unrealistic counterfactuals, making them unsuitable for healthcare applications, and is limited by the need for multiple calls to an optimization module. Although CFVAE [Nagesh et al., 2023] was designed for generating counterfactuals in healthcare settings using variational autoencoders, it does not account for realistic challenges in healthcare, such as class imbalance in rare disease cases and missing values in datasets. To overcome these limitations, we propose a novel method designed for healthcare applications, particularly in rare disease diagnosis. Our approach generates personalized counterfactuals for clinicians while handling missing values and class imbalance in the training data.

B Experimental Datasets

To evaluate our method, we consider the following three private datasets.

Gitelman Syndrome This dataset comprises real clinical records from a top hospital, focusing on Gitelman syndrome (GS), a rare autosomal recessive renal tubulopathy. The data contains 594 patients, including 94 diagnosed with GS and 500 non-GS individuals. Five key diagnostic features are included: *Serum Potassium*, *Urine Potassium*, *pH*, *Bicarbonate*, and *High Blood Pressure*, with labels derived from clinical diagnoses. To emulate real-world scenarios where critical test results are missing (a common challenge in rare disease diagnosis), we retain the missing values in the original data. This enables counterfactual analysis to quantify how missing tests impact predictions, thereby guiding clinicians to prioritize specific examinations for undiagnosed cases. The dataset is split into 80%-20% train-test sets for GS classification, with subsequent counterfactual perturbation analysis performed in the latent space of the complete data. It should be noted that we retained the situation of data imbalance, which is to be consistent with the situation that the incidence of rare diseases in the real world is much lower. And despite this imbalance, our model still maintained good performance.

Acromegaly This dataset includes real-world clinical records from a top hospital, focusing on acromegaly, a chronic disorder caused by excessive growth hormone (GH) secretion, typically due to pituitary somatotroph adenomas. The data contains 181 patients, comprising 88 diagnosed with acromegaly and 93 non-acromegaly controls. Three clinically significant features are incorporated: *Serum GH*, *IGH-1*, and *OGTT-GH_min*, with labels derived from clinical diagnoses. To reflect realistic data incompleteness, we retain naturally occurring missing values in the original dataset and explicitly record their positions. This facilitates counterfactual generation that aligns with clinical practice, allowing clinicians to evaluate how incomplete laboratory profiles influence diagnostic predictions.

The dataset is partitioned into 80%-20% training-test sets for binary classification, followed by counterfactual perturbation and interpretability analysis in the latent space of the complete data to identify critical diagnostic drivers.

Hypertrophic Cardiomyopathy (HCM) This dataset includes real-world clinical records from a top hospital, focusing on hypertrophic cardiomyopathy (HCM), an inherited cardiac disorder characterized by abnormal myocardial thickening that may lead to ventricular outflow tract obstruction, arrhythmias, and heart failure. The data contains 36 patients, including 21 HCM-diagnosed individuals and 15 individuals with another rare disease (ATTR, amyloidosis trans-thyretin related) as the control group. Eight clinically significant features are incorporated: *Asymmetric Hypertrophy*, *SAM*, *Low Left Ventricular Voltage*, *High Left Ventricular Voltage*, *Family History*, *Sarcomere Gene Mutation*, *TTR Gene Mutation*, and *Amyloid Deposition*. Similarly, to preserve clinical authenticity, naturally occurring missing values in the original dataset are retained and explicitly mapped for interpretability. The dataset is partitioned into 80%-20% training-test splits for HCM classification. Post-training, counterfactual perturbation and causal analysis are conducted in the latent space of the complete data to identify critical diagnostic patterns and feature interactions.

Granulomatosis with Polyangiitis (GPA) This dataset, relevant to the context of the file s13023-019-1040-6.pdf, is derived from [Chen et al., 2024] and contains real-world clinical records targeting granulomatosis with polyangiitis (GPA), which is an ANCA-associated vasculitis frequently linked to PR3-ANCA and upper-airway/pulmonary involvement. The cohort includes 93 subjects in total, comprising 11 patients diagnosed with GPA and 82 non-GPA controls that are deliberately selected for their high clinical confusability with GPA in ENT (ear, nose, and throat) and respiratory presentations; it incorporates seven clinically meaningful binary features, namely *Otitis Media*, *Hemoptysis*, *Proteinase 3 Antibody Titer, Elevated (PR3-ANCA)*, *Cytoplasmic ANCA (c-ANCA) Present*, *Knee Pain (Bilateral)*, *Peripheral Cyanosis (one month to one year)*, and *Rhinitis*, with labels derived from clinical diagnoses. The dataset is split into an 80%-20% training–test partition for binary GPA classification, with naturally occurring missing values retained and their positions mapped; subsequent to the classification task, counterfactual perturbation and interpretability analysis are conducted in the latent space of the completed data to identify key diagnostic drivers and interactions between symptoms and serological indicators.

C Rationale for Choosing Masked Denoising Autoencoder (mDAE): A Comparison with Other Autoencoder Variants

To clarify why the Masked Denoising Autoencoder (mDAE) is selected for our framework rather than other autoencoder variants, we conduct a comparative analysis of Deterministic Autoencoder (AE), Variational Autoencoder (VAE), Denoising Autoencoder (DAE), and their derivatives, with a focus on their suitability for rare disease diagnostic scenarios:

Deterministic Autoencoder (AE) AEs lack mechanisms to handle noise or missing values, which are common in rare disease data. They overfit to sparse inputs, producing unreliable latent representations and counterfactuals, making them unsuitable.

Variational Autoencoder (VAE) VAEs, as generative models, center on modeling the joint distribution information. Furthermore, their inherent stochasticity in latent spaces hinders precise, targeted counterfactuals needed to correct cognitive anchoring, often generating implausible clinical values and propagating biases via heuristic imputation of missing data, which limits clinical utility.

Denoising Autoencoder (DAE) and Masked Denoising Autoencoder (mDAE) DAEs are explicitly designed to process corrupted or incomplete inputs, with a focus on modeling $p(\text{missing } \mathbf{x} \mid \text{observed } \mathbf{x})$. Standard DAEs enhance noise robustness but lack dedicated handling of missing data (a common challenge in rare disease), **a gap our masked DAE (mDAE) fills** by explicitly training on partially observed data via sparse masks to reconstruct complete profiles. It generates deterministic latents for precise control over counterfactual perturbations and enforces physiological constraints to ensure clinically valid outputs in rare disease scenarios.

D Counterfactual Sample Generation

To address the challenges and diagnostic needs in rare disease medicine, our model supports counterfactual analysis across diverse scenarios. In this section, we present three representative and practically relevant scenarios for detailed evaluation.

Scenario 1: Feature Completion for Low-Confidence Predictions: When a patient's original input features have missing values, overlap significantly with common disease characteristics, and yield low-confidence AI predictions for common diagnoses, our model generates counterfactual samples to address missing features. This refines clinical judgments and guides decision-making.

Scenario 2: AI-Human Prediction Discrepancy Resolution: In situations where AI predictions diverge from clinician diagnoses, our model produces counterfactual "flipped" samples to highlight the underlying differences in decision-making logic. These samples provide interpretable evidence that helps clinicians reconcile inconsistent conclusions.

Scenario 3: Uncertainty-Driven Alternative Diagnoses: By perturbing feature vectors in latent spaces where clinicians exhibit maximal diagnostic uncertainty, our model generates alternative diagnosis lists. This anchors cognitive bias correction and supports robust differential diagnosis.

E Counterfactual Sample Generation

To address the challenges and diagnostic needs in rare disease medicine, our model supports counterfactual analysis across diverse scenarios. In this section, we present three representative and practically relevant scenarios for detailed evaluation.

Scenario 1: Feature Completion for Low-Confidence Predictions: When a patient's original input features have missing values, overlap significantly with common disease characteristics, and yield low-confidence AI predictions for common diagnoses, our model generates counterfactual samples to address missing features. This refines clinical judgments and guides decision-making.

Scenario 2: AI-Human Prediction Discrepancy Resolution: In situations where AI predictions diverge from clinician diagnoses, our model produces counterfactual "flipped" samples to highlight the underlying differences in decision-making logic. These samples provide interpretable evidence that helps clinicians reconcile inconsistent conclusions.

Scenario 3: Uncertainty-Driven Alternative Diagnoses: By perturbing feature vectors in latent spaces where clinicians exhibit maximal diagnostic uncertainty, our model generates alternative diagnosis lists. This anchors cognitive bias correction and supports robust differential diagnosis.

F Training Configuration Details

F.1 Hyperparameter and loss weight selection

All hyperparameters and loss weights were selected via a systematic grid search confined strictly to the training set, ensuring that the independent 20% test set remained untouched throughout model development and thereby preventing data leakage.

Within the 80% training set, we adopted a hold-out validation strategy: 70% of the data were used for model fitting, and the remaining 30% served as a validation subset to evaluate hyperparameter configurations.

- **Learning rate** was searched over the range $[10^{-5}, 10^{-3}]$.
- **Most loss function weights** were searched over a clinically relevant range of $[0.1, 2.0]$.
- **Mask sparsity loss weight**, due to its role as a regularization term requiring finer control to balance sparsity constraints and model performance, was searched over the narrower range of $[10^{-5}, 0.1]$.

Searches were guided by validation AUC, with priority given to configurations demonstrating stable performance (AUC variance < 0.02) across three random seeds. The final hyperparameters and loss weights were chosen based on the best validation AUC while ensuring model outputs remained within clinically plausible ranges.

F.2 Stage-Wise Training Details

The model is trained in four stages: DAE warm-up, AI predictor training, joint human predictor and mask network training, and fine-tuning. Table 3 specifies the learning rate schedules, batch sizes, and regularization strategies (e.g., gradient clipping) for each phase on the Gitelman syndrome dataset. For instance, the DAE warm-up phase employs learning rate annealing and early stopping to stabilize latent space initialization. This staged approach balances model complexity and training stability while ensuring task-specific optimization.

Table 3: Progressive training strategy

Phase	**Components**	**Learning Rate**	**Key Details**
DAE Train	Encoder / Decoder	1e-4	• LR annealing • Early stop • Gradient clip ≤ 1.0 • Batch size 16
AI Predictor Train	AI Predictor Network	1e-4	• LR annealing • Early stop • Gradient clip ≤ 1.0 • Batch size 16
Human Predictor + Mask Net Train	Human Predictor Network, Mask Network	1e-4	• LR annealing • Early stop • Gradient clip ≤ 1.0 • Batch size 16
Fine-Tuning	Full Network	1e-4	• Gradient clip ≤ 1.0 • Batch size 16

F.3 Loss Function Weight in Fine-Tuning Stage

The total training loss combines multiple objectives, including reconstruction, classification, contrastive separation, and cognitive gap minimization. Table 4 defines the weights assigned to each loss component on the Gitelman syndrome dataset, emphasizing the balance between feature reconstruction (dominant in early stages) and rare/common disease separability (enforced via contrastive loss).

Table 4: Loss Function Specification

Loss Type	**Weight**	**Function**
Reconstruction	1	Reconstruct input features
AI	1	Maximize AI prediction accuracy
Human	1	Align with human diagnoses
Mask	0.001	Promote sparse attention masks masks
Contrastive	1.5	Separate rare/common diseases
Gap	1.5	Reduce human-AI attention gaps

G Model Architecture Details

G.1 DAE Architectures

The Denoising Autoencoder (DAE) architecture captures clinical feature mappings through an Encoder and Decoder. The Encoder uses ELU activations to project raw features into a 32-dimensional latent space, while the Decoder reconstructs inputs from this space. Categorical features are embedded via a dedicated layer, and the design supports robust learning from incomplete data. Take the Gitelman syndrome dataset as an example, key components are detailed in Table 5, which outlines layer dimensions and functional roles.

Table 5: DAE architecture configuration

Component	**Layers**	**Dimension**	**Functional Description**
Encoder	Input Layer	5	Raw clinical features
	Hidden Layer	128	ELU-activated transformation: $h = \text{ELU}(Wx + b)$
	Latent Space	32	Bottleneck representation: z
	Embedding	8	Categorical feature encoding: $\text{onehot}(x)W_e$
Decoder	Input Layer	32	Latent space input: z
	Hidden Layer	128	Feature decoding: $h_d = \text{ELU}(W_d z + b_d)$
	Output Layer	5	Feature reconstruction: $\hat{x}$

G.2 Predictor Architectures

The AI and human predictors, along with the attention mask network, are designed to explicitly model the divergence between machine and clinician reasoning. The AI predictor operates in the full latent space to generate ground truth-aligned diagnoses, while the human predictor uses a sparse attention mask (generated by the mask network) to simulate cognitive constraints in clinical decision making. Table 6 outlines the architecture details, including layer dimensions, activation functions, and the attention mechanisms. This modular design supports interpretable counterfactual generation by isolating human-AI cognitive gaps in the latent space.

Table 6: Predictor Architectures Configuration

Component	Layers	Dim/Num of Heads	Description
AI Predictor	Input Layer	32	ELU-activated projection into hidden space
	Hidden Layer	128	ELU transformation of latent features
	Output Layer	2	Produces class logits for prediction
Mask Network	Input Layer	5	ELU-activated linear embedding
	Attention Layer	4	Multi-head self-attention for contextual feature interaction
	Output Layer	32	Generates masking coefficients
Human Predictor	Input Layer	32	Takes the masked latent representation as input
	Hidden Layer	128	ELU transformation of masked latent space
	Output Layer	2	Produces class logits aligned with experts

H Broader Impact and Limitation

This study aims to address the underdiagnosis of rare diseases caused by cognitive biases in clinical decision-making. Our framework helps clinicians consider rare conditions more effectively through generative counterfactuals, potentially reducing diagnostic delays and improving patient outcomes, especially in underserved areas with limited specialized expertise. By modeling the cognitive gaps between humans and AI, it promotes transparent and bias-aware collaboration, setting a practical example for AI applications in healthcare and other high-stakes fields. Potential risks include the possibility of over-relying on AI, which we mitigate by designing interpretable counterfactual explanations to supplement, rather than replace, clinical judgment.

One key limitation of this study stems from the long-standing challenge of rare disease data acquisition and sharing, a core bottleneck in rare disease research. Unlike common disease domains with accessible public datasets, there is a severe scarcity of open, high-quality data resources for rare diseases. To address this gap, our team invested over a year in close collaboration with a top-tier hospital, engaging multiple departments and relying on substantial clinician effort—to construct three private rare disease datasets tailored to this research. However, due to strict ethical and privacy constraints, these datasets cannot be fully made public. To alleviate this limitation in the future, we aim to develop and release a rare disease data simulator: this tool will generate synthetic data with characteristics consistent with real rare disease cases, supporting the reproducibility of related research while upholding privacy protection requirements.

I Computing Infrastructure

All synthetic data experiments are performed on Ubuntu 20.04.3 LTS system with Intel(R) Xeon(R) Gold 6248R CPU @ 3.00GHz, 227 Gigabyte memory.